USING RESOURCE BASED SLICING TO CAPTURE THE INTERMITTENCY OF VARIABLE RENEWABLES

Mariliis Lehtveer, Niclas Mattsson, Fredrik Hedenus, Martin Soini

Physical Resource Theory, Chalmers University of Technology, SE-412 96, Gothenburg, Sweden

*Corresponding author: mariliis.lehtveer@chalmers.se, +46 317 723 129

ABSTRACT

As the share of variable renewables – wind and solar PV – is expected to grow significantly in coming decades, it has become increasingly important to account for their intermittency in large scale energy models that are used to explore long term energy futures. In this paper we propose and evaluate one method for doing so, namely, resource based slicing. In addition we implement storage based on possible transitions between slices which allows us to explore new dynamics between intermittent generation and electricity storage in large scale models. Our preliminary results show that this approach manages to capture many aspects introduced by variable renewables such as need for flexible generation capacity and curtailment at high penetration levels. We show that adding electricity storage to the system will favour solar power but has only a minor effect on wind and nuclear power.

Keywords: Variability, renewable energy sources, energy system model, time slices

1. Introduction

If global warming is to be kept under 2°C with reasonable certainty, greenhouse gas (GHG) emissions must drop by roughly half by mid-century compared to current levels and continue to decline afterwards [1]. The power system is one of the main sources of emitted anthropogenic GHGs accounting for about 30% of the total emissions [2], and therefore one of the main targets for emission reductions. Many possibilities exist for supplying energy with low life cycle emissions such as the use of biomass, wind, solar, hydro or nuclear power. There are, however, many challenges related to significant expansion of those sources. Hydro and biomass resources are limited and do not suffice to fulfil the growing global energy demand [3]. Nuclear power brings along radioactive waste production, accidental radiation release risk, nuclear weapons proliferation risk and public opposition to expansion [4-6]. These caveats have led many to the conclusion that nuclear power does not have a place in the future energy system as exemplified by recent decisions in Germany, Belgium and Switzerland to phase out nuclear power [7], and thus its future is uncertain. Solar and wind power have a vast physical resource potential but only supply a small share of current global energy production due to high costs [3]. However, recent years have seen large cost reductions for both wind and solar photovoltaic (PV) technologies and also increased investments [8]. Therefore it is likely that these technologies will play a major role in the future electricity system if the 2-degree target is to be met.

Yet large scale expansion of wind and solar power brings along another set of challenges. The supply from wind and solar PV technologies is variable in both short and long term and not reliably predictable. Thus large amounts of wind and solar power complicate systems operation by changing the residual load shape, increasing the uncertainty of supply and increasing the need for ramping reserves. Therefore, if significant amounts of this type of capacity is installed in the system, there may be an oversupply of electricity at windy and sunny times which is likely to result in low or even negative electricity prices. This in turn will diminish revenues for variable renewables as electricity prices tend to be low when they are able to produce electricity, and also for baseload due to decreased and more unpredictable running times. Thus the amount of solar and wind generation in the system will have a large influence on all investment decisions in the system and on the total cost of the system. This effect will become more acute with increasing penetration of wind and solar.

Long-term energy models representing multiple sectors and regions are often used to investigate the questions related to long term developments such as decarbonisation of the energy system. These models typically make a cost-effective choice among large number of technologies and optimise investment decisions over many time periods and over vast geographic area. This makes these models computationally demanding and simplifications in temporal, geographic and technical detail are necessary to maintain reasonable running-times. Typically time steps of 5-10 years are modelled in such models [9]. However, supply from wind and solar varies on much shorter time scales and is thus difficult to capture in this type of models.

Traditionally, models such as GET [10] often circumvent this problem by simply limiting the amount of variable renewables to 25-30% of electricity production; a level that is widely viewed as possible to integrate into current systems without significant additional costs. This approach limits the role that variable renewables can play in scenarios designed to investigate possible pathways to global climate mitigation, and therefore model results can be misleading. Different approaches have been tried by various modelling groups to avoid this artificial restriction and incorporate intermittency related effects into long-term energy models. For example, Sullivan et al. use additional constraints to capture the capacity credit provided by different penetration levels of intermittent renewables as well as technology dependent flexibility coefficients to account for the increased need for back-up capacity and flexible generation as the penetration of variable renewables increases [11]. Another approach is to interlink long-term capacity expansion models with short-term dispatch models [12]. However, this method requires considerable effort to set up both models and ensure the convergence of their results, as well as extensive additional computational resources.

The infeed from wind and solar is not the only source of variability in the power system – the demand for electricity is also fluctuating over time. To capture the variability of demand in large energy system models, a time slice approach is often used. This involves implementing a coarse load duration curve for electricity demand, in which hours with similar levels of demand are grouped together (typically day/night, week-day/week-end, and seasons). Recently, attempts have been made to extend this approach also to variable renewable sources. For example, Ludig et al. investigate the effect of increased time resolution of demand based slicing on capturing the variability of renewables and find that it helps to better capture the variability of demand and solar infeed, but does not adequately represent the variability of wind infeed [13]. Nahmmacher et al. propose an approach for selecting representative days and summarise other attempts in that direction [9]. They find 6 representative days with 3 hour resolution to be sufficient to reflect the characteristic fluctuations in input data. Yet this approach results in 48 time slices that may make it inapplicable for large scale energy models due to high computational requirements.

In this paper we propose another solution for representing variability of wind and solar PV in large scale energy models based on resource based slicing.

2. Method

2.1. GET model

We perform this analysis using the Global Energy Transition (GET) model first developed by Azar and Lindgren [14] and further developed in Hedenus et al. [10]. GET is a cost minimizing "bottom-up" systems engineering model of the global energy system set up as a linear programming problem. The model was constructed to study carbon mitigation strategies over a 100-year period with an objective of meeting both a specified energy demand and a carbon constraint while minimising the discounted total energy system cost for the period under study (in general 2000–2100). In our analysis we build on the version 8.0 of GET, featuring improved representation of the nuclear cycles. For more detail please see Lehtveer and Hedenus [15].

The model focuses on the supply side and has five end use sectors: electricity, transport, feedstock, residential–commercial heat and industrial process heat. In each sector various technologies are available to meet the demand. Technologies are described by the energy carriers they can potentially convert, and are parameterised using e.g. investment and variable costs, efficiencies, load factors and carbon emissions. Demand projections are based on the MESSAGE B2 scenarios based on increasing global population, intermediate levels of economic development and a stabilisation level of 480 ppm CO_2-eq by 2100 [16].Transportation demand scenarios are based on Azar et al. [14] and assume faster efficiency improvements in the transport sector than in the B2 scenario. The model has perfect foresight and thus finds the least cost solution for the entire study period with a discount rate of 5%. Consequently, scarce resources such as oil and biomass are allocated endogenously to the sectors in which they are used most cost-effectively. The resource base for non-variable sources was updated for this model version based on [3] and [17].

In the model version developed in this paper, GET 9.0, the world is divided into 10 regions including North America (NAM), Europe (EUR), Pacific OECD (PAO), centrally planned Asia (CPA), the former Soviet Union (FSU), Latin America (LAM), Africa (AFR), the Middle East (MEA), South Asia (SAS) and non-OECD Pacific Asia (PAS) following IIASA region definitions with the exception of Europe where we have joined Eastern and Western Europe into one region. The countries and territories belonging to each region are listed in Appendix B. We construct the mitigation pathways for all regions meeting the 450 ppm CO_2 target globally based on the idea of contraction and convergence [18] using a climate sensitivity of 3ºC per doubling of CO_2. The developed regions and emerging economies roughly halve their emissions compared to the baseline by 2050, whereas developing regions (AFR, MEA, SAS, PAS) reduce emissions by 35% compared to the baseline. From 2060 we assume a global cap, and emissions are allocated among regions in the most cost-effective way.

The diffusion of technologies is limited so that no technology can increase or decrease its market share by more than 20% in 10 years in any specific sector such as electricity or centralised heat production; nor can the installed capacity for a technology increase by more than 30% per year. For developing technologies, investment costs decline linearly over the 2010-2050 period and reach mature levels as indicated in Table 1. More information about the model framework can be found in [15].

Table 1. Investment costs of technologies in GET model. Sources: [19-21]

Technology	Starting cost per kW ($ 2010)	Mature cost per kW ($ 2010)	Load factor	Efficiency
Coal PP	1800	1800	0.8	45%
Coal with CCS	3000	2500	0.8	35%
Gas turbine	800	800	0.8	55%
Gas with CCS	2000	1500	0.8	45%
Concentrated solar power (CSP)	12750	7000	0.7	N/A
Light water reactor (LWR)	7000	5000	0.8	33%
Fast breeder reactor (FBR)	8500	6000	0.8	41%
Wind	2100	1500	N/A	N/A
Solar PV	3000	1000	N/A	N/A
Storage 12h	1800	1200	N/A	80%
Storage 48h	2900	1900	N/A	80%
Storage 2w	6200	3900	N/A	80%
Storage 2m	11600	7200	N/A	80%

2.2. Slicing wind and solar production

To analyse the availability of wind and solar resources we retrieve global temporally resolved raw data for wind speeds and solar irradiation from the ECMWF ERA Interim dataset with the geographic resolution of 0.5°x0.5° [22]. For wind power, the data is then converted to absolute wind speeds 125 meter above ground and for the solar PV technology the average irradiation is projected globally onto solar panels with a tilt equal the latitude of the respective location. All data sets are filtered by population density to avoid the allocation of wind power in highly populated areas and to allocate solar PV preferentially to urban areas. Furthermore, only locations within 500km of populated areas are considered suitable for both wind and solar power development.

For each region we construct a production profile of wind and solar. To do so we allocate an amount of energy from either source to a region based on the region's electricity demand in 2100. The actual investment made is, however, determined by the optimisation model in a later stage. The production profile is an aggregate of local load factors of chosen pixels and depends on where wind or solar capacity is allocated. The allocation is based on average potential output of the location as well as proximity to populated areas. In addition we assume that some geographical spread of capacity is required due to grid limitations and political considerations.

To account for this we set a maximum capacity density of 250 kW per km^2 for wind power and divide each region into 3 to 10 clusters based on size of the region, and then allocate wind and solar PV capacity in proportion to a combination of the population of each cluster and its resource quality. A more detailed description of the process is presented in the Appendix A.

The resulting data is used to create 10 time slices based on solar and wind load factors in each region. Nine time slices are created by combining low, medium and high solar categories with low, medium and high wind categories. The tenth slice is intended to capture extremely low wind situations; it is created by further dividing the low wind and low solar slice into two, based on load factors for wind. Resulting load factors for slices are displayed in Table 2, and slice lengths (i.e. the share of hours that fall into each slice) in Table 3. Although demand is not used as an input for slicing, the daytime demand (i.e. slices with medium and high solar) is assumed to be 15% higher than night-time demand based on ENTSO-E 2014 data for Europe [23]. This difference is assumed to be the same for all regions. In the current version of the model, time slices have only been implemented for electricity generation. The use of electricity in other sectors such as heat or transport is limited to be proportional to the demand and the slice length.

Furthermore, an additional constraint is introduced to take into account start-up and ramping limitations of thermal technologies and restrictions on the use of hydro reservoirs. To prevent these technologies from ramping down to zero, they must always run at a minimum share of their actual output in any other time slice. These shares are displayed in Table 4.

Table 2. Load factors for different time slices and regions obtained from the global wind and solar data analysis.

		Low solar, low wind	Low solar, medium wind	Low solar, high wind	Medium solar, low wind	Medium solar, medium	Medium solar, high wind	High solar, low wind	High solar, medium wind	High solar, high wind	Low solar, extremely low wind
Wind	**AFR**	0.19	0.27	0.38	0.18	0.27	0.38	0.18	0.26	0.36	0.11
Wind	**CPA**	0.12	0.23	0.39	0.10	0.23	0.39	0.11	0.23	0.38	0.07
Wind	**EUR**	0.13	0.24	0.44	0.13	0.24	0.44	0.12	0.23	0.42	0.08
Wind	**FSU**	0.21	0.32	0.48	0.20	0.32	0.48	0.18	0.31	0.47	0.11
Wind	**LAM**	0.22	0.32	0.44	0.20	0.32	0.45	0.20	0.32	0.45	0.13
Wind	**MEA**	0.21	0.30	0.41	0.17	0.29	0.40	0.19	0.29	0.38	0.13
Wind	**NAM**	0.21	0.34	0.49	0.20	0.33	0.49	0.19	0.33	0.48	0.12
Wind	**PAO**	0.21	0.31	0.42	0.20	0.30	0.41	0.20	0.30	0.41	0.12
Wind	**PAS**	0.12	0.19	0.35	0.11	0.19	0.35	0.11	0.18	0.34	0.06
Wind	**SAS**	0.08	0.17	0.47	0.07	0.18	0.46	0.07	0.18	0.45	0.04
Solar	**AFR**	0.01	0.01	0.01	0.26	0.26	0.26	0.64	0.64	0.64	0.01
Solar	**CPA**	0.01	0.01	0.01	0.26	0.26	0.26	0.57	0.57	0.57	0.01
Solar	**EUR**	0.00	0.00	0.00	0.14	0.14	0.14	0.49	0.49	0.49	0.00
Solar	**FSU**	0.01	0.01	0.01	0.16	0.16	0.16	0.41	0.41	0.41	0.01
Solar	**LAM**	0.01	0.01	0.01	0.26	0.26	0.26	0.62	0.62	0.62	0.01
Solar	**MEA**	0.02	0.02	0.02	0.27	0.27	0.27	0.62	0.62	0.62	0.02
Solar	**NAM**	0.00	0.00	0.00	0.16	0.16	0.16	0.53	0.53	0.53	0.00
Solar	**PAO**	0.00	0.00	0.00	0.11	0.11	0.11	0.56	0.56	0.56	0.00
Solar	**PAS**	0.01	0.01	0.01	0.28	0.28	0.28	0.61	0.61	0.61	0.01
Solar	**SAS**	0.00	0.00	0.00	0.25	0.25	0.25	0.63	0.63	0.63	0.00

Table 3. Length of time slices obtained from the global wind and solar data analysis.

	Low solar, low wind	Low solar, medium wind	Low solar, high wind	Medium solar, low wind	Medium solar, medium wind	Medium solar, high wind	High solar, low wind	High solar, medium wind	High solar, high wind	Low solar, extremely low wind
AFR	0.131	0.233	0.174	0.109	0.105	0.054	0.107	0.063	0.023	0.001
CPA	0.138	0.289	0.170	0.081	0.101	0.058	0.047	0.067	0.037	0.011
EUR	0.110	0.266	0.183	0.064	0.131	0.098	0.051	0.077	0.017	0.003
FSU	0.128	0.239	0.145	0.068	0.130	0.080	0.104	0.071	0.032	0.002
LAM	0.143	0.231	0.170	0.117	0.093	0.050	0.096	0.065	0.033	0.002
MEA	0.088	0.297	0.196	0.106	0.073	0.015	0.109	0.097	0.016	0.002
NAM	0.162	0.212	0.130	0.130	0.106	0.059	0.112	0.051	0.017	0.021
PAO	0.120	0.205	0.174	0.117	0.090	0.044	0.117	0.089	0.041	0.002
PAS	0.154	0.298	0.140	0.082	0.108	0.054	0.053	0.076	0.030	0.005
SAS	0.158	0.312	0.135	0.093	0.063	0.040	0.106	0.054	0.030	0.009

Table 4. Share of maximum output that must be run during the whole time period if technology is used.

	Aggregate part-load
Biomass PP	0.35
Oil PP	0.1
Gas PP	0.1
Coal PP	0.35
LWR	0.7
FBF	0.7
MOX	0.7
Hydro PP	0.1

2.3. *Modelling electricity storage*

As high penetration of variable renewables increases the variability of electricity prices due to the oversupply at windy and sunny times and shortage of supply options at less windy and sunny times, storing electricity and releasing it during the time of high demand or low variable infeed is likely to become an attractive feature of the energy system. Unfortunately most of the time information is lost in the slicing approach we explore, which complicates the modelling of electricity storage. However, some information relevant for operation of storage can be regained by analysing the original wind and solar data at high time resolution. Every storage technology has a characteristic storage time, sometimes called the energy-to-power ratio. For every hour of wind and solar resource data, we look ahead a number of hours corresponding to the characteristic storage time and note the time slice each hour was allocated to. This results in the number of hours per year that an electricity transfer between each time slice is possible. This method is similar to the transition matrix approach proposed by Wogrin et al. [24]. Table 5 shows the number of hours that transfer between different slices in possible in North America (NAM) region. For example, low solar and medium wind slice will follow high solar and medium wind slice within a 12 hour time period 111 hours per year. Currently only one year of data is used to estimate the possible transfer times.

In our model we study four different lengths of storage: 12 hours, 48 hours, 2 weeks and 2 months. The costs for 12 and 48 hour storage are based on the cost data for pumped hydro storage obtained from Zakeri and Syri [20]. For longer storage times our costs are not based on real data and serve here only to test the modelling approach.

Table 5. Transfer matrix for 12 hours storage in North America (NAM) in number of hours the transfer between slices is possible per year.

From \ To	Low solar, low wind	Low solar, medium wind	Low solar, high wind	Medium solar, low wind	Medium solar, medium wind	Medium solar, high wind	High solar, low wind	High solar, medium wind	High solar, high wind	Low solar, extremely low wind
Low solar, low wind	771	137	2	288	8	0	199	8	0	7
Low solar, medium wind	56	1012	114	125	293	15	143	96	2	0
Low solar, high wind	0	55	657	0	96	209	2	65	55	0
Medium solar, low wind	275	143	2	436	29	0	203	12	0	39
Medium solar, medium wind	12	280	77	41	366	14	49	89	2	0
Medium solar, high wind	0	16	191	1	20	234	0	18	39	0
High solar, low wind	227	92	2	223	23	0	359	2	0	58
High solar, medium wind	14	111	45	5	95	11	12	152	0	0
High solar, high wind	0	8	49	0	2	35	0	4	53	0
Low solar, extremely low wind	61	2	0	21	0	0	20	0	0	80

2.4. Sensitivity analysis

To analyse the robustness of obtained results we perform a sensitivity analysis of the costs of some key technologies: solar PV, wind power, nuclear power and electricity storage. For wind, solar PV and nuclear we specified four cost levels reflecting possible mature costs reached by 2050. The cost for wind power also includes investment in extra grid capacity, estimated based on Holttinen et al [25]. For electricity storage technologies three cost levels were specified and additionally a case with no storage available. The costs are summarised in Table 6. The costs of both nuclear technologies and the four storage technologies are varied together since it is assumed that the same cost reduction mechanisms will affect all variants of these technologies. The model was then solved for all possible combinations of solar PV, wind, nuclear and electricity storage costs, resulting in 256 model runs.

Table 6. Mature costs of technologies in sensitivity analysis.

Costs in US$(2010)	Level I	Level II	Level III	
Wind	2100	1800	1500	
Solar PV	1500	1200	850	
LWR	6250	5000	3750	
FBR	7500	6000	4500	
Storage 12h	No storage	1200	900	
Storage 48h	No storage	1900	1350	
Storage 2w	No storage	3900	2500	
Storage 2m	No storage	7200	4500	

3. Results

3.1. Basic results

For comparison with the 10-slice model described above, we also run a version of the model with only a single time slice, using average wind and solar PV capacity factors. Although the standard version of the GET model limits electricity generation from intermittent sources to a maximum of 25% of total electricity supply, this constraint was deactivated for the single-slice runs performed here. For each model version we run both a scenario without carbon constraints ("baseline") and also a scenario with 450ppm CO_2 concentration target. For the basic runs in this section, no other electricity storage than hydrogen is available. We present here only results for the electricity system, but we reiterate that our model encompasses all sectors of the energy system.

Figure 1 compares global electricity generation in the single slice model with the nine-slice model. The difference between the two models is relatively small in the baseline scenario, which is mostly based on thermal electricity production. The main difference can be seen in the last two decades of the century in which solar is used instead of wind in the ten-slice version. At the same time the use of gas is reduced in the single slice model whereas its share stays significant in the 10 slice version. This reflects the correlation between higher daytime demand and solar electricity production as well as the use of gas for peak power. Using wind or thermal generation for the higher demand would result in idle capacity for a large part of the year and thus expensive. However, this effect is saturated relatively quickly and thus wind power that can also produce during the night becomes more cost-effective. In the single slice version of the model this dynamic is lost and wind is chosen due to a lower production cost.

However differences become much more significant when carbon emissions are constrained, thus increasing the competitiveness of low carbon electricity sources such as wind and solar power (figure 2). In the single slice version, wind power dominates the system and reaches 86% of the electricity supply by 2100, being outcompeted only by hydro power. There is a minor contribution from solar PV of about 1% of electricity supply by 2100. Thus, the total share of variable electricity production is 87% by year 2100. In our sliced version, the electricity mix is much more heterogeneous; 47% of produced electricity in 2100 comes from wind power and 14% from solar PV, i.e. a total variable production share of about 61%. Additionally, significantly more gas power is used in the sliced model run.

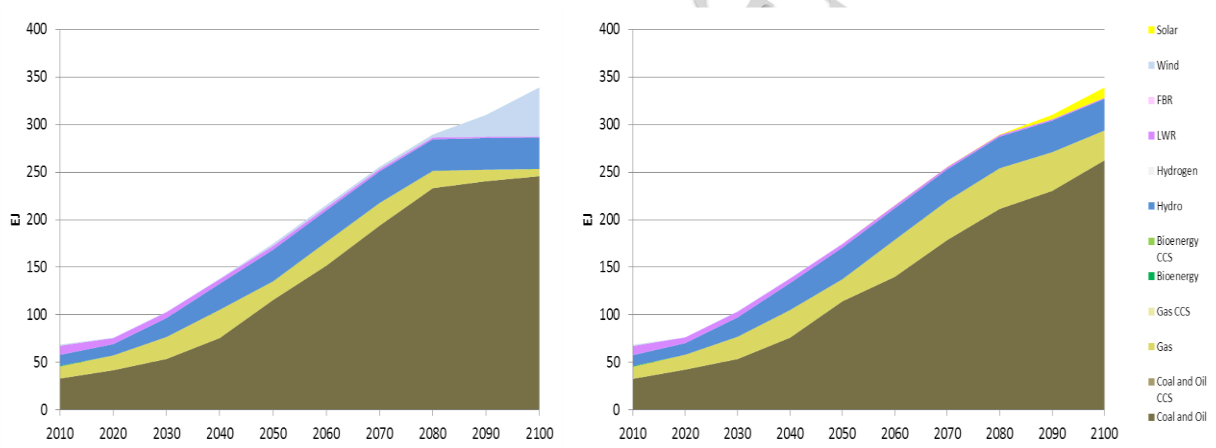

Figure 1. Global electricity production - baseline scenario with one slice (left) and ten slices (right).

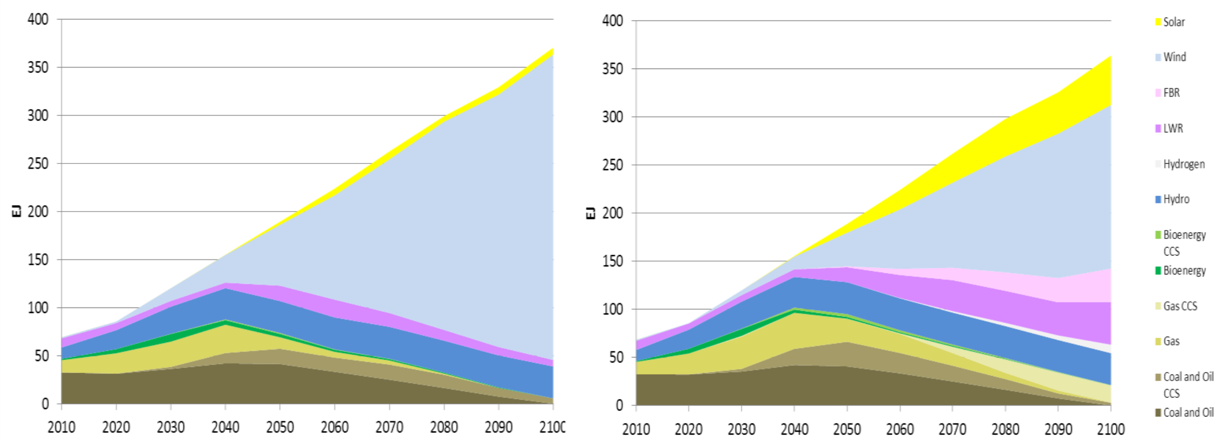

Figure 2. Global electricity production – 450 ppm CO_2 scenario one slice (left) and ten slices (right).

Figures 3 and 4 show the electricity production mix in Europe and Africa over different time slices in 2050 and 2100. Note the interplay between the varying resource availability in different slices and the constraints on thermal and hydro generation, and how the least-cost production system involves some "over-investment" in capacity of variable renewables and occasionally curtailing excess generation. If wind power is available at sufficiently low cost, it may be cost effective to accept some curtailment during the windiest conditions in order to have more capacity when wind is less abundant. In 2050 when wind penetration is relatively low, wind is not curtailed and flexible capacity (gas and hydro) is used instead to meet the demand. In 2100, emission budgets are more stringent and less fossil fuels can be used. Since Carbon Capture and Storage (CCS) is not entirely carbon free in our model – only 95% of the emissions are captured – its use is limited at the end of the century. The main competition therefore will be between nuclear, wind and solar technologies as they do not emit any CO_2 in our model. With our default cost assumptions, the result is a large share of wind power along with some curtailment, moderated by some use of electricity storage using hydrogen (no other storage is available here). It is also interesting to note that in 2050, coal power with CCS is chosen by the model in Europe, whereas in Africa coal power without CCS is used simultaneously. This is caused by our climate scenario set up that allocates a larger emission budget to developing countries. However, a global cap is assumed starting in 2060.

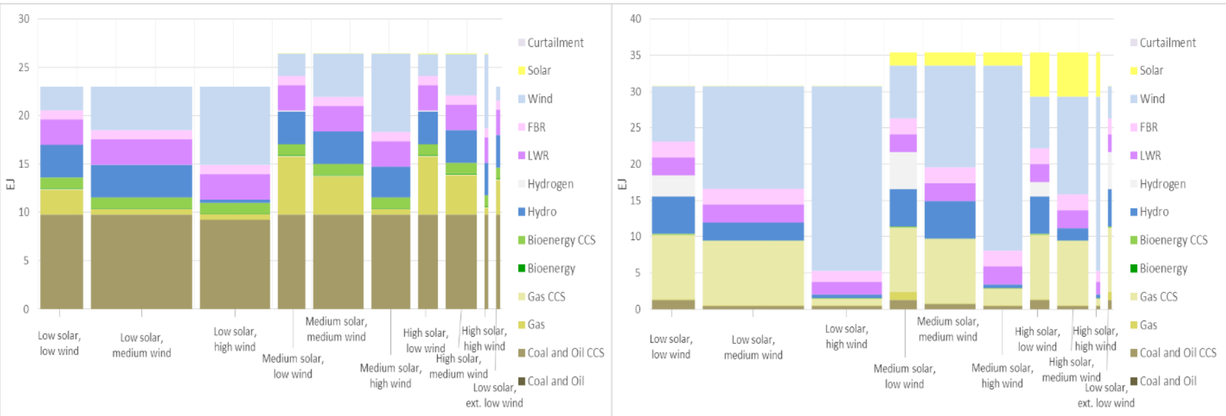

Figure 3. Electricity production mix in different slices for Europe in 2050 (left) and 2100 (right) with the 450 ppm CO_2 scenario. The width of the slice represents the share of hours that fall into this category. No storage technologies other than hydrogen are enabled in these runs.

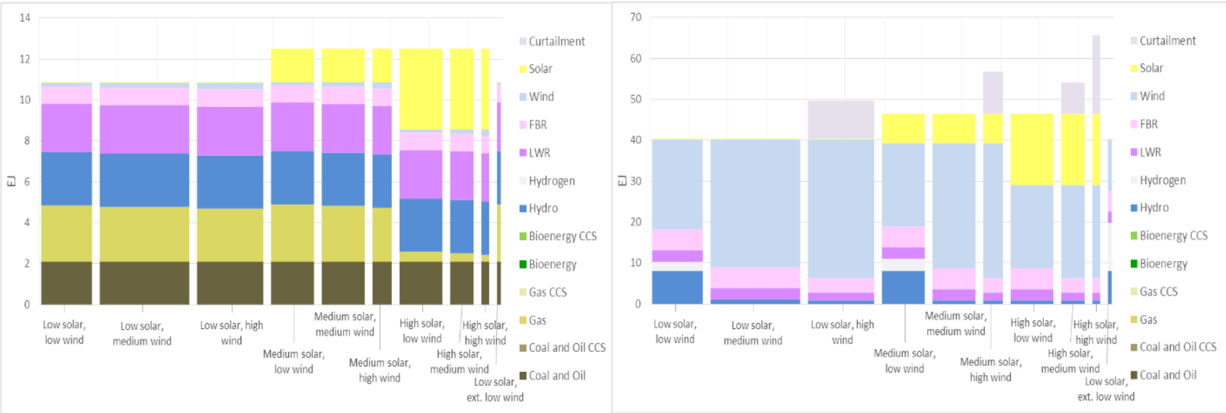

Figure 4. Electricity production mix in different slices for Africa in 2050 (left) and 2100 (right) with the 450 ppm CO_2 scenario. The width of the slice represents the share of hours that fall into this category. No storage technologies other than hydrogen are enabled in these runs.

Finally we note that the regions end up with very different shares of low emitting electricity sources in their supply (see Figure 5). This is caused by the difference in resource quality among the regions and is reflected in our regional load factors (c.f. table 2). Thus Southern Asia (SAS and PAS) with low quality wind resources is dominated by nuclear supply whereas regions well-endowed with wind such as EUR and NAM feature mainly renewables based systems.

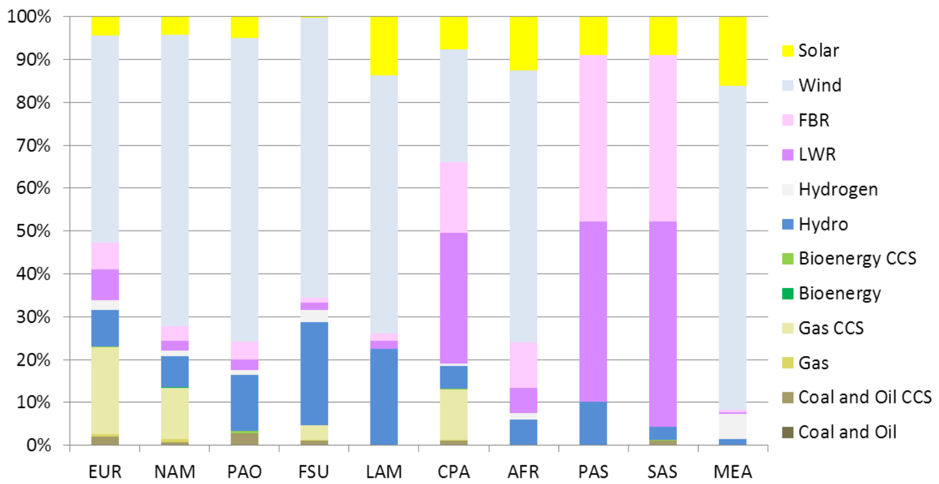

Figure 5. Regional electricity production mixes in 2100 in 450 ppm CO_2 scenario.

3.2. *THE EFFECT OF STORAGE*

Enabling the storage option in the model allows for electricity transfers between slices but this option is not always used due to high cost and also due to limited transfer possibilities between slices (as described in section 2.3 above). For storage to be cost-effective it needs to be cycled relatively often, resulting in relatively high capacity factor. In Europe, long windy periods are often followed by rather long low wind periods. Therefore, the transfer possibilities from high wind slices to low infeed slices are limited. They are also costly because they require longer storage times, and therefore storage is not employed even at 2100 as shown on figure 6.

In Africa, solar is used to a higher extent because there is a large potential to regularly transfer energy from day to night, which makes short-term storage economically attractive. Therefore enabling electricity storage results in a significant reduction of curtailment measured as lost potential electricity generation (from 3.1 EJ/yr to 0.4 EJ/yr or from 7% to 1% of regions electricity production). The production from solar PV increases by 3.4 EJ or 60% and the production from wind and nuclear power is reduced by 1.7EJ/yr and 1 EJ/yr accordingly.

Globally the effect of storage is small on the modelled cost level. The use of gas is decreased by 3% and wind and nuclear technologies by 1.3% each by availability of storage. Solar power sees the biggest change with 9.5% increase. Only 24 and 48 hour storage technologies are employed at this cost level. For the long term electricity storage hydrogen is used.

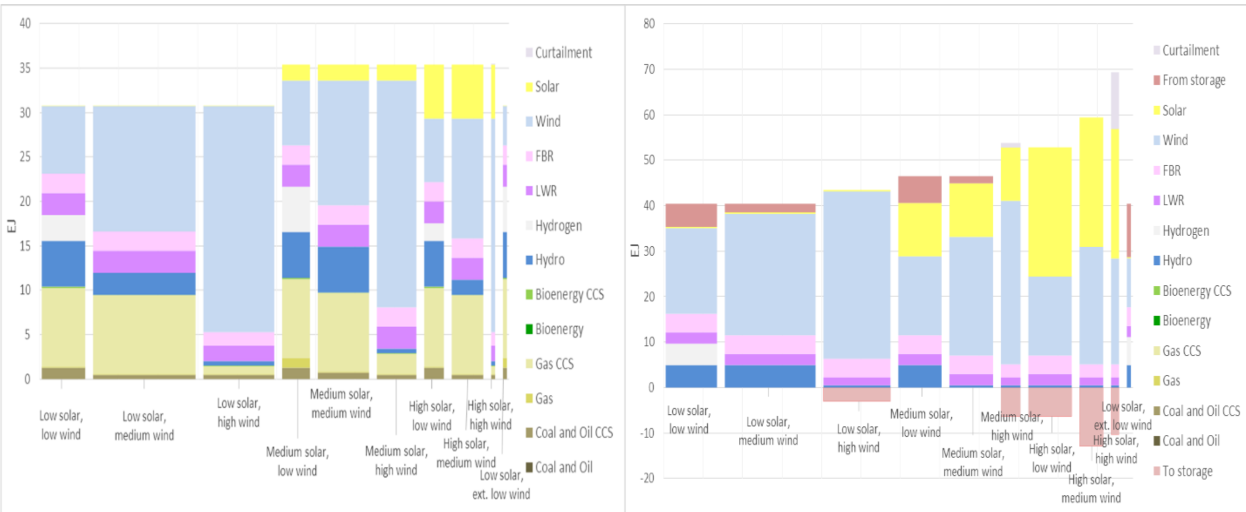

Figure 6. Electricity production mix in different slices for Europe (left) and Africa (right) in 2100 with electricity storage enabled and with the 450 ppm CO_2 scenario. The width of the slice represents the share of hours that fall into this category.

3.3. Sensitivity analysis

To investigate the robustness of our basic results we varied the cost of nuclear, wind and solar PV technologies as well as storage as described in section 2.4 and solved our model for 256 different combinations of these costs. Results for 2070 are shown in Figure 7.

Without storage availability solar PV never exceeds 32% of the global electricity supply in our model and averages 9% over all runs. The penetration of wind and nuclear power is more cost sensitive and ranges from 0-51% for wind and 2-69% for nuclear power, with averages of 16% and 38% respectively. Enabling storage options has a very limited effect on wind and nuclear power but increases the potential penetration of solar PV significantly. With the least expensive storage costs, solar PV can reach up to 52% of total electricity production. However, the average penetration of solar PV remains at 13% regardless of the availability and costs of storage. In contrast, the average penetration of nuclear power is reduced by inexpensive storage by 3 percentage units. Average wind penetration is not affected. Additionally, inexpensive storage enables larger electrification of other sectors and increases the supply of electricity by 1% on average but by 4% in most extreme cases. In most run the result is a mix of solar, wind and nuclear technologies in electricity supply, only in the case of high costs for others and low cost for one the cheaper technology dominates. However, without the storage solar PV will never dominate the global supply. The tendency to a portfolio of technologies rather than a dominance of a single one is a result of varying regional resource quality.

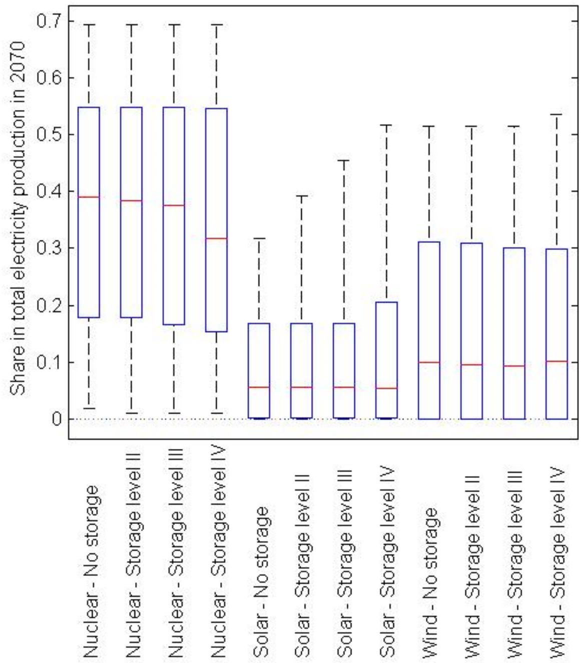

Figure 7. Share of different sources in electricity production in 2070. Black bars represent the range, blue boxes middle 50% of the results and red lines the median results.

4. Discussion

Our results show that resource based slicing can capture characteristic aspects of variability, such as the trade-off between curtailment during high availability and supplying significant amount of electricity during lower availability, the interplay with flexible and inflexible thermal plants, and the benefits of different lengths of electricity storage.

Yet, many assumptions and simplifications have been made in the current application of the method. First, the input data for slicing variable renewables is based on only one year of global data. However, wind and solar patterns vary somewhat from year to year and are also expected to change due to global warming. For this reason the load factors we derive from our solar and wind data, and hence our results, would change somewhat if more data were available. Similarly, for our analysis of storage technologies, the hours during which transfer between different slices is possible is also likely to vary slightly from year to year. Further analysis of the robustness of data used in this study and its effect on results is needed. We emphasise that the results presented in this paper serve only to illustrate the method.

In addition, our current approach does not divide wind and solar resources into different classes. A single average load factor is given to all investments in any given region (although the load factor varies between regions and time slices). Thus, for an investment at a very good site, there is also implicitly an investment in a not so good site. In reality some locations in any region have a better resource quality than others, with corresponding higher load factors. Investment in only such locations can occur even if their potential is relatively small compared to the energy demand of the region. This is not captured in our current modelling. However, it would be relatively straightforward to combine our resource-based slices with varying classes of wind and solar resources.

We do not explicitly model the grid extensions needed for large scale renewable penetration. Yet when the production profiles are constructed we implicitly assume significant amounts of new transmission capacity are needed at a uniform grid cost per kW of wind power installed in all regions. In reality this cost is likely to vary depending on the penetration of variable renewables, pre-existing infrastructure and grid design.

Similarly to any other slicing method, modelling a limited number of slices results in a large degree of averaging. Each slice shown in this analysis includes hours with quite different wind and solar infeed. Also demand fluctuations are not accounted for in our analysis. However, if data is available demand could be included in slice creation as done by Wogrin et al. [24]. This however is likely to result in a larger number of slices and would increase the computational requirements.

In our model we impose a ramping constraint that thermal technologies and hydro power if employed must run at least a certain share of their maximum output in any other slice. This constraint is also likely to affect the results from our model and thus further work testing robustness of chosen values is required.

Although the method presented in this paper is relatively simple and can relatively easily be implemented in large scale energy models, it fails to adequately represent all the aspects related to large scale penetration of variable renewables. Wogrin et al. test the method of grouping similar systems states and using a transition matrix to describe interactions between states similar to our approach, and find that although this method gives more accurate results than time based slicing in technology deployment and electricity price, it still tends to underestimate peak prices and overestimate off-peak prices of electricity [24]. This should be kept in mind while using this method to answer electricity price related research questions.

Another question is how to model electricity trade in this set up. In our model version there is no electricity trade between model regions and therefore each region can be sliced independently. However, if our method is to be applied to more detailed models in which interregional electricity trade plays a role, two different approaches can be applied. First, it is possible to slice the whole modelled area at the same time. Due to regional differences in wind and solar production at any given time this approach would result in larger averaging of wind and solar load factors. Another possible approach is to use transition matrices similar to the ones used here to model storage but to count for simultaneous high supply/low supply hours where electricity trade is economically attractive.

In addition, losing time information makes it more difficult to take into account load changes from heat and transport sectors. Again, some of that information could be regained by using the transition matrix approach. Alternatively, these sectors could also be sliced based on availability of variable renewables.

5. Conclusions

As the share of variable renewables – wind and solar PV – is expected to grow significantly in coming decades, it has become increasingly important to account for their intermittency in large scale energy models that are used to explore long term energy futures. In this paper we propose and evaluate one method for doing so, namely, resource based slicing. By analysing global wind speed and solar insolation data we derive load factors for different wind and solar situations in 10 world regions, and use this data as input to the Global Energy Transition (GET) model. Since even a small number of resource based time slices are sufficient to capture the variability of solar and wind power, this enables us to remove traditional constraints on intermittent electricity generation from the model. In addition we implement storage based on possible transitions between slices which allows us to explore new dynamics between intermittent generation and electricity storage in large scale models.

Our preliminary results show that this approach manages to capture many aspects introduced by variable renewables such as need for flexible generation capacity and curtailment at high penetration levels. We also find optimal electricity production mixes to vary significantly between regions due to different endowments of solar and wind resources. We show that adding electricity storage to the system will favour solar power but has only a minor effect on wind and nuclear power. However, our approach is aimed at large integrated assessment type models, and the simplistic implementation is unable to capture all intermittency related issues. As always, the suitability of the method depends on the research question one wants to answer.

Acknowledgements

We would like to thank ÅF and Chalmers Area of Advance Energy for funding this research project.

References

1. Rogelj, J., et al., *Emission pathways consistent with a 2°C global temperature limit.* Nature Climate Change, 2011. **1**(8): p. 413-418.
2. Institute, W.R., *Climate Analysis Indicator Tool*.
3. Rogner, H.-H., et al., *Chapter 7 - Energy Resources and Potentials*, in *Global Energy Assessment - Toward a Sustainable Future*. 2012: Cambridge University Press, Cambridge, UK and New York, NY, USA and the International Institute for Applied Systems Analysis, Laxenburg, Austria. p. 423-512.
4. Sagan, S.D., *The causes of nuclear weapons proliferation.* Annual Review of Political Science, 2011. **14**: p. 225-244.
5. von Hippel, F., et al., *Chapter 14 - Nuclear Energy*, in *Global Energy Assessment - Toward a Sustainable Future*. 2012: Cambridge University Press, Cambridge, UK and New York, NY, USA and the International Institute for Applied Systems Analysis, Laxenburg, Austria. p. 1069-1130.
6. HPS, *Radiation and Risk: Expert Perspectives*. 2013, Health Physics Society.
7. Rogner, H.H., *World outlook for nuclear power.* Energy Strategy Reviews, 2013. **1**(4): p. 291-295.
8. IEA, *World Energy Outlook 2014.* 2014.
9. Nahmmacher, P., et al., *Carpe diem: A novel approach to select representative days for long-term power system models with high share of renewable energy sources*. 2014, USAEE

10. Hedenus, F., et al., *Cost-effective energy carriers for transport - The role of the energy supply system in a carbon-constrained world.* International Journal of Hydrogen Energy, 2010. **35**(10): p. 4638-4651.
11. Sullivan, P., V. Krey, and K. Riahi, *Impacts of considering electric sector variability and reliability in the MESSAGE model.* Energy Strategy Reviews, 2013. **1**(3): p. 157-163.
12. Deane, J.P., et al., *Soft-linking of a power systems model to an energy systems model.* Energy, 2012. **42**(1): p. 303-312.
13. Ludig, S., et al., *Fluctuating renewables in a long-term climate change mitigation strategy.* Energy, 2011. **36**(11): p. 6674-6685.
14. Azar, C., K. Lindgren, and B.A. Andersson, *Global energy scenarios meeting stringent CO2 constraints - Cost-effective fuel choices in the transportation sector.* Energy Policy, 2003. **31**(10): p. 961-976.
15. Lehtveer, M. and F. Hedenus, *Nuclear Power as a Climate Mitigation Strategy – Technology and Proliferation Risk.* Journal of Risk Assesment, 2013.
16. IIASA, *GGI Scenario database*.
17. McGlade, C. and P. Ekins, *The geographical distribution of fossil fuels unused when limiting global warming to 2 [deg]C.* Nature, 2015. **517**(7533): p. 187-190.
18. Höhne, N., M. den Elzen, and M. Weiss, *Common but differentiated convergence (CDC): A new conceptual approach to long-term climate policy.* Climate Policy, 2006. **6**(2): p. 181-199.
19. MIT, *The Future of the Nuclear Fuel Cycle: an Interdiciplinary MIT Study.* 2011.
20. Zakeri, B. and S. Syri, *Erratum: Electrical energy storage systems: A comparative life cycle cost analysis (Renew. Sustain. Energy Rev. (2015) 42 (569-596)).* Renewable and Sustainable Energy Reviews, 2016. **53**: p. 1634-1635.
21. Lehtveer, M. and F. Hedenus, *Nuclear power as a climate mitigation strategy - technology and proliferation risk.* Journal of Risk Research, 2014.
22. *ERA Interim dataset*. 2014, ECMWF - European Centre for Medium-Range Weather Forecasts.
23. *Consumption Data - Hourly Load Values*. 2014, ENTSO-E - European Network of Transmission System Operators for Electricity.
24. Wogrin, S., et al., *A new approach to model load levels in electric power systems with high renewable penetration.* IEEE Transactions on Power Systems, 2014. **29**(5): p. 2210-2218.
25. Holttinen, H., et al., *Impacts of large amounts of wind power on design and operation of power systems, results of IEA collaboration.* Wind Energy, 2011. **14**(2): p. 179-192.

Appendix A - Analysis of global solar and wind data

To construct a reasonable approximation of a potential future distribution of wind and solar power a multi-step process is implemented. The overarching target is the allocation of wind and solar plants at sites featuring good primary resources, while at the same time avoiding an overly optimistic concentration at the regional hot spots. The rationale behind this approach consists in the technical and political limitations to a globally optimal allocation, e.g. given by electric grid constraints or the separate clean energy targets in independent countries.

Data origin and conversion

Solar and wind data for the year 2014 with a resolution of 6 hours is retrieved from the ERA Interim data set of the European Centre for Medium-Range Weather Forecasts with a geographic resolution of 0.5°×0.5° covering the whole surface of the planet. This yields a grid of 720 pixels in longitude and 361 pixels in latitude with varying surface area. The calculated output from solar plants is based on the SSRD parameter with 3 hour resolution, which is converted to direct normal irradiation and projected globally onto hypothetical photovoltaic solar panels facing south/north on the northern/southern hemisphere at a tilt angle equal the latitude of the respective geographic location. The calculation of the onshore wind power is based upon the data with 6 hour resolution of the U and V components of the wind speeds for the ERA model level 57 out of 60, corresponding to an altitude of roughly 125 meters above ground. The absolute wind speed values are converted to wind turbine power output using the profile of a "future low-land wind farm" [2].

Data filtering

The calculation of the temporally and geographically resolved data in units of kWh/yr/m^2 (photovoltaics) and m/s (wind power) is followed by two filtering steps to make the final allocation more realistic:

1 The filtering of the pixels according to population density serves to exclude highly populated locations (in the case of onshore wind power) and too remote locations, and to give urban regions a preferential treatment in the allocation of photovoltaic capacity. Based on the CIESIN "Population Density Grid Future Estimates, v3" dataset for the year 2015 with a 0.5° resolution [3] the pixels with "low population density" (<10/km^2)

and "high population density" (>500/km^2) where identified. Furthermore, all pixels within 500 km of a pixel with population density of >10/km^2 are deemed suitable for the construction of wind and solar farms.

2 All coordinates with yearly average wind speed <5m/s are excluded from the subsequent processing.

The following table gives an overview of the filtering applied to each technology

Population density [1/km^2]	**PV**	**Wind onshore**
<10	Within 500 km	Within 500 km, if speed >5m/s
10< and <500	Yes	Yes, if speed >5m/s
>500	Preferred	No

Clustering

In each region the pixels deemed suitable for the accommodation of wind/solar capacity are grouped into individual sub-regions (clusters). The allocation of certain amounts of capacity to each of the sub-regions serves as an approximate representation of the limited real-world grid-connectivity within the region.

A standard k-means algorithm is employed to cluster the pixels in such a way to minimise the sum of squares of the pixels' coordinates within each of these sub-regions. The choice for this particular approach is motivated by the k-means algorithm's tendency to produce similarly sized clusters. The number of clusters and the initial mean values of the corresponding pixels' positions are defined manually to ensure the reproducibility of the result.

Allocation

The allocation to the individual clusters is based on the weighted fractions of the clusters' total population (30%) and total solar and wind resource availability (70%). This emphasis on the resource availability serves to avoid the unrealistic excessive allocation in highly populated clusters with poor resource endowment.

Finally, the cluster capacity is assigned to the comprising pixels: For each cluster the pixels are ranked according to their yearly energy production, for wind and solar power separately. The best sites are then chosen successively until the cumulative output equals the cluster's allocated energy production. For wind power, a base capacity of 250 kW/km^2 is assumed. The ratio of PV panel area to land area was chosen to be 2.5%, in order to obtain a reasonable spread. The radiation-to-AC efficiency of PV is assumed to be 15%. In the case of photovoltaics, capacity is preferentially allocated to (urban) pixels with high population density to take into account the possibility of integrating this technology into the built environment.

Generation of representative hourly capacity factor curves for each region

Once the pixels for the allocations have been chosen, the technology-specific cumulative hourly capacity factors can be calculated from the temporally resolved input data. For each region this is done by summing the hourly generated energy on all sites and normalising it accordingly to obtain the hourly capacity factor.

[1]European Centre for Medium-Range Weather Forecasts, ERA Interim dataset, http://apps.ecmwf.int/datasets/data/interim-full-daily/

[2]J R. McLean, "*Equivalent Wind Power Curves*", D2.4 deliverable, www.trade-wind.eu, 2007.

[3] Center for International Earth Science Information Network - CIESIN - Columbia University, and Centro Internacional de Agricultura Tropical - CIAT. 2005. Gridded Population of the World, Version 3 (GPWv3): Population Density Grid, Future Estimates. Palisades, NY: NASA Socioeconomic Data and Applications Center (SEDAC). http://dx.doi.org/10.7927/H4ST7MRB. Accessed 11 May 2015.

[4] "5-minute Gridded Global Relief Data (ETOPO5)," U.S. Department of Commerce, National Oceanic and Atmospheric Administration. http://iridl.ldeo.columbia.edu/SOURCES/.NOAA/.NGDC/.ETOPO5/datasetdatafiles.html. Accessed 11 May 2015

Appendix B – Definition of regions

Sub-Saharan Africa (AFR): Angola, Benin, Botswana, British Indian Ocean Territory, Burkina Faso, Burundi, Cameroon, Cape Verde, Central African Republic, Chad, Comoros, Cote d'Ivoire, Congo, Djibouti, Equatorial Guinea, Eritrea, Ethiopia, Gabon, Gambia, Ghana, Guinea, Guinea-Bissau, Kenya, Lesotho, Liberia, Madagascar, Malawi, Mali, Mauritania, Mauritius, Mozambique, Namibia, Niger, Nigeria, Reunion, Rwanda, Sao Tome and Principe, Senegal, Seychelles, Sierra Leone, Somalia, South Africa, Saint Helena, Swaziland, Tanzania, Togo, Uganda, Zaire, Zambia, Zimbabwe

Centrally planned Asia and China (CPA): Cambodia, China (incl. Hong Kong), Korea (DPR), Laos (PDR), Mongolia, Viet Nam

Europe (EUR): Albania, Andorra, Austria, Azores, Belgium, Bosnia and Herzegovina, Bulgaria, Canary Islands, Channel Islands, Croatia, Czech Republic, Cyprus, Denmark, Faeroe Islands, Estonia, Finland, France, The former Yugoslav Rep. of Macedonia, Germany, Gibraltar, Greece, Greenland, Hungary, Iceland, Ireland, Isle of Man, Italy, Latvia, Lithuania, Liechtenstein, Luxembourg, Madeira, Malta, Monaco, Netherlands, Norway, Poland, Portugal, Romania, Slovak Republic, Slovenia, Spain, Sweden, Switzerland, United Kingdom, Turkey.

Former Soviet Union (FSU): Armenia, Azerbaijan, Belarus, Georgia, Kazakhstan, Kyrgyzstan, Republic of Moldova, Russian Federation, Tajikistan, Turkmenistan, Ukraine, Uzbekistan (the Baltic republics are in the Central and Eastern Europe region)

Latin America and the Caribbean (LAC): Antigua and Barbuda, Argentina, Bahamas, Barbados, Belize, Bermuda, Bolivia, Brazil, Chile, Colombia, Costa Rica, Cuba, Dominica, Dominican Republic, Ecuador, El Salvador, French Guyana, Grenada, Guadeloupe, Guatemala, Guyana, Haiti, Honduras, Jamaica, Martinique, Mexico, Netherlands Antilles, Nicaragua, Panama, Paraguay, Peru, Saint Kitts and Nevis, Santa Lucia, Saint Vincent and the Grenadines, Suriname, Trinidad and Tobago, Uruguay, Venezuela)

Middle East and North Africa (MEA): Algeria, Bahrain, Egypt (Arab Republic), Iraq, Iran (Islamic Republic), Israel, Jordan, Kuwait, Lebanon, Libya/SPLAJ, Morocco, Oman, Qatar, Saudi Arabia, Sudan, Syria (Arab Republic), Tunisia, United Arab Emirates, Yemen

North America (NAM): Canada, Guam, Puerto Rico, United States of America, Virgin Islands

Pacific OECD (PAO): Australia, Japan, New Zealand

Other Pacific Asia (PAS): American Samoa, Brunei Darussalam, Fiji, French Polynesia, Gilbert-Kiribati, Indonesia, Malaysia, Myanmar, New Caledonia, Papua, New Guinea, Philippines, Republic of Korea, Singapore, Solomon Islands, Taiwan (China), Thailand, Tonga, Vanuatu, Western Samoa

South Asia (SAS): Afghanistan, Bangladesh, Bhutan, India, Maldives, Nepal, Pakistan, Sri Lanka